Francesco BECATTINI<sup>1</sup>, Francesco POGGI<sup>1\*</sup>, Luca TANTERI<sup>2</sup>, Pierluigi CONFUORTO<sup>1</sup>, Matteo DEL SOLDATO<sup>1</sup>, Sandro MORETTI<sup>1</sup>, Federico RASPINI<sup>1</sup>

# Open-source InSAR data for the characterization of geomorphic processes at different scales

Abstract: Becattini F., Poggi F., Tanteri L., Confuorto P., Del Soldato M., Moretti S., Raspini F., Open-source InSAR data for the characterization of geomorphic processes at different scales. (IT ISSN 0391-9838, 2025). Ground deformation, such as landslides and land subsidence, is a prevalent and potentially hazardous phenomenon in a multitude of landscapes. It is imperative to comprehend the nature and extent of ground movement to ensure the safety of individuals, infrastructure, and natural environments. The advent of satellite-based radar technology and related services has facilitated the observation of ground motion across extensive regions with exceptional precision and continuity. Among these, the European Ground Motion Service (EGMS) provides free and standardized displacement measurements that are increasingly utilised in geomorphological studies. The present paper includes an automated methodology to extract and classify ground deformation patterns from EGMS data. The objective is to support large-scale geomorphological analysis and hazard assessment. A fully automated procedure has been developed and applied to identify clusters of ground motion across Italy. Two different velocity thresholds (±10 mm/year and ±5 mm/year) were used to test their influence on detection and classification. The application of the higher threshold resulted in the identification of over 2,000 clusters, while the lower threshold led to the identification of almost 10,000 clusters. These results highlight the systematic capability of the method to detect and classify different deformation processes across the national scale. The results obtained demonstrate that steeper slopes exhibiting horizontal movement are commonly associated with landslides, while vertical motion in flat areas is indicative of subsidence. Local case studies confirmed the ability of the method to detect both strong and subtle deformation signals, even in complex or urbanized environments and its capability to support characterization of deformation pattern. The findings demonstrate that open satellite data, when combined with automated tools, enhances the mapping and interpretation of surface deformation both at national and local scales. The method is scalable from local to national applications and can be adapted to other European regions to support land management, early warning, and long-term monitoring strategies.

Key words: Landslide, Remote sensing, Interferometry, Open data, Geomorphological mapping.

Riassunto: Becattini F., Poggi F., Tanteri L., Confuorto P., Del Soldato M., Moretti S., Raspini F., Dati InSAR open source per la caratterizzazione dei processi geomorfologici a diverse scale. (IT ISSN 0391-9838, 2025). La deformazione del suolo, come le frane e la subsidenza, rappresenta un fenomeno diffuso e potenzialmente pericoloso in numerosi contesti paesaggistici. Comprendere la natura e l'entità dei movimenti del terreno è fondamentale per garantire la sicurezza delle persone, delle infrastrutture e degli ambienti naturali. L'avvento delle tecnologie radar satellitari e dei servizi ad esse collegati ha reso possibile l'osservazione dei movimenti superficiali su ampie aree con eccezionale precisione e continuità. Tra questi, l'European Ground Motion Service (EGMS) fornisce gratuitamente misure standardizzate di spostamento, sempre più utilizzate negli studi geomorfologici. Il presente lavoro propone una metodologia automatizzata per estrarre e classificare i pattern di deformazione del suolo a partire dai dati EGMS, con l'obiettivo di supportare analisi geomorfologiche su larga scala e la valutazione della pericolosità. È stata sviluppata e applicata una procedura completamente automatica per identificare cluster di movimento del terreno sull'intero territorio italiano. Sono state testate due diverse soglie di velocità (±10 mm/anno e ±5 mm/anno) per valutarne l'influenza sul rilevamento e sulla classificazione: l'applicazione della soglia più alta ha permesso di individuare oltre 2000 cluster, mentre quella più bassa ha portato all'identificazione di quasi 10 000 cluster. Questi risultati evidenziano la capacità sistematica del metodo di rilevare e classificare diversi processi deformativi su scala nazionale. Le analisi mostrano che i versanti più ripidi con movimenti orizzontali sono comunemente associati a frane, mentre i movimenti verticali in aree pianeggianti sono indicativi di subsidenza. I casi studio locali hanno confermato la capacità del metodo di rilevare segnali di deformazione sia marcati che deboli, anche in contesti complessi o urbanizzati, e di supportare la caratterizzazione dei pattern deformativi. I risultati dimostrano che i dati satellitari open, se combinati con strumenti automatici, migliorano la mappatura e l'interpretazione della deformazione superficiale sia a scala nazionale che locale. Il metodo è scalabile dalle applicazioni locali a quelle nazionali e può essere adattato ad altre regioni europee per supportare la gestione del territorio, i sistemi di allerta precoce e le strategie di monitoraggio a lungo termine.

Termini chiave: Frana, Telerilevamento, Interferometria, Dati aperti, Cartografia geomorfologica.

<sup>&</sup>lt;sup>1</sup> Department of Earth Sciences, University of Firenze, Firenze, Italy.

<sup>&</sup>lt;sup>2</sup> Civil Protection Centre, University of Firenze, Firenze, Italy.

<sup>\*</sup>Corresponding author: Francesco Poggi (francesco.poggi1@unifi.it)

#### INTRODUCTION

Geomorphological mapping is a key component of geosciences and aims to identify, classify and describe processes and landforms. In recent decades, geomorphologic mapping has evolved from a purely field-based exercise aimed at accurate representation of landforms to highly interpretative maps at various scales, mainly based on digital remote sensing data (Knight et al., 2011). In this sense, the assessment of geomorphological features has become more quantitative, making it possible to obtain both spatial and temporal information, and leading it to play an increasingly important role in supporting engineering geology (Hearn, 2019; Laimer, 2021). To this, Synthetic Aperture Radar Interferometry (InSAR) data is nowadays a consolidated tool for mapping a wide range of landforms, such as periglacial and alpine landforms (Eckerstorfer et al., 2018; Strozzi et al., 2020; Hu et al., 2023), sinkholes (Gutiérrez et al., 2011; Busetti et al., 2020), faults activity (Murgia et al., 2019; Lazos et al., 2022) and mass movements (Solari et al., 2020; Confuorto et al., 2023; Famiglietti et al., 2024). Moreover, especially with the technological development of more complex and robust processing techniques and with the launch of Sentinel-1, which has been providing continuous data worldwide since 2014, InSAR has proven to be a fundamental tool for small up to very large-scale analyses of the deformation. In fact, several post-processing techniques have been developed in recent years that aim to filter InSAR information from millions of measurement points and identify the potentially most dangerous movements. The first approaches relied on fast methods such as hot-spot-like approaches (Meisina et al., 2008; Bianchini et al., 2012; Lu et al., 2012; Barra et al., 2017) or are based on cluster analysis (Montalti et al., 2019; Tomás et al., 2019; Solari et al., 2020). A more complex method is the ADA (Active Deformation Area) tools (Navarro et al., 2020), which semi-automatically extract and provisionally interpret the areas affected by the deformation detected by InSAR. Festa et al. (2022) developed the MAC (Moving Area Cluster) to detect and classify clusters of deformation at a national level in Italy. More recently, Tiwari and Shirzaei (2024) developed an automated semi-supervised Machine-Deep-Learning approach to detect hotspot signals of deformation in Los Angeles (USA) area. Nowadays, at a European level, InSAR data are provided for free through the EGMS (European Ground Motion Service) providing consistent A-DInSAR data at a continental scale (Crosetto et al., 2020). Since its launch several studies have used such data for the mapping of landforms: Medici et al. (2025) analysed the landslides in Great Britain, Parenti et al. (2024) for studying landslides in Emilia Romagna (Northern Apennines, Italy), Torre et al. (2024) made a comprehensive analysis of landslides in the coastal sector of La Herradura, Southern Spain. However, multi-hazard mapping at national level using EGMS data is still lacking. Several of these existing approaches, although

valuable, present limitations when applied to large-scale and standardized datasets. ADA tools (Navarro et al., 2020) require semi-automatic processing and parameter tuning, which can reduce reproducibility and scalability. The MAC algorithm (Festa et al., 2022) was successfully applied in Italy, but relies on user-defined criteria and limited validation, making its systematic application less straightforward. Other methods, such as PSI-HCA (Tomás et al., 2019; Solari et al., 2020), integrate interferometric results with ancillary information but are computationally demanding and mostly restricted to Permanent Scatterer datasets. Compared to these approaches, the methodology presented here is fully automated, reproducible, and designed to operate consistently at both national and local scales by exploiting standardized EGMS products. Here in this paper, we use a clustering approach to detect and classify ground motions occurring in Italy using EGMS data. The interferometric data were accessed, downloaded, and converted using the EGMStream web application (Becattini et al., 2025), a tool specifically designed to facilitate the handling of EGMS products. The nationwide identification of moving areas serves as a screening phase to analyse specific landform dynamics through further post-processing tools capable of interpreting deformation time series. Two case studies, Bosmatto (Aosta Valley) and Castagnola (Liguria), were selected to evaluate and discuss the capability of the method to describe local-scale deformation patterns in detail and to validate the classification results in different geomorphological contexts.

### DESCRIPTION OF THE STUDY AREAS

Italy presents a highly complex and dynamic geological and geomorphological framework, shaped by the long-lasting interaction between the African and Eurasian tectonic plates (Doglioni, 1991; Vai and Martini, 2001). This convergence has given rise to a wide range of tectonic structures and lithological domains, resulting in an extremely articulated topography and a high degree of geodiversity.

From a geological perspective, the Italian territory includes three main structural domains: the Alpine chain in the north, the Apennine range extending along the peninsula, and the magmatic and volcanic districts located in central and southern Italy and on the islands (Bortolotti and Principi, 2005). The Alps represent a classic example of a collisional orogen, characterized by high relief, crystalline and metamorphic basement rocks, and active gravitational processes such as deep-seated landslides and rockfalls (Agliardi *et al.*, 2009). The Apennines, largely composed of sedimentary sequences, are shaped by compressional and extensional tectonics, and host a variety of shallow landslides, earth flows, and complex slope movements, often affecting inhabited areas and infrastructure networks (Soldati and Marchetti, 2017).

In addition, several intermontane and coastal basins, such as the Po Plain in the north and the alluvial plains of Campania and Apulia in the south, are affected by subsidence phenomena, both natural and anthropogenic, often related to groundwater overexploitation, sediment compaction, and tectonic lowering (Carminati and Martinelli, 2002; Del Soldato *et al.*, 2018). Volcanic areas, such as Vesuvius, Campi Flegrei, Etna, and the Aeolian Islands, are subject to a combination of uplift, subsidence, and slope deformation driven by magmatic and hydrothermal activity.

Geomorphologically, the territory includes high mountains, steep slopes, badlands, river valleys, terraced coasts, and karst plateaus, each associated with specific types of ground motion and landscape evolution processes (Panizza, 1996). These diverse settings, combined with intense anthropogenic pressure and a dense historical settlement pattern, make Italy one of the countries most exposed to hydrogeological and geomorphological hazards in Europe (Trigila *et al.*, 2007; ISPRA, 2022). The overall morphotectonic structure and topographic variability of the country are effectively represented in fig. 1, which shows a shaded digital elevation model (DEM) of the entire Italian territory.

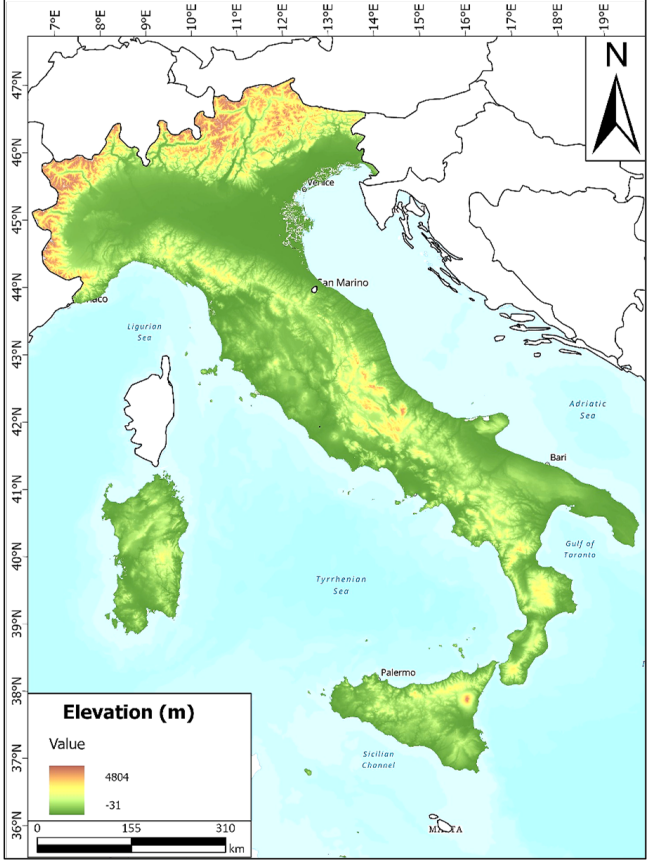


Figure 1 - Shaded digital elevation model (DEM) of Italy, showing the main topographic gradients and morphotectonic regions. The visualization emphasizes the elevation variability across mountain chains, basins, and coastal plains.

This high variability of geological and morphological conditions makes Italy an ideal context for testing large-scale automated methods of ground motion classification based on remote sensing data. The national-scale analysis presented in this work thus aims to explore the spatial distribution of active deformation processes and assess the capability of EGMS data to support systematic geomorphological investigations across a wide range of natural settings.

#### The Bosmatto landslide

The Bosmatto landslide is an ancient landslide localized in the municipality of Gressoney-Saint-Jean in Valle d'Aosta Region (Northwestern Alps, Italy). More precisely, the landslide is located on the west-facing slope of the glacial Lys Valley crossed by the homonymous River. The slopes of this area are quite steep (30 to 40 degrees), and from a geological point of view the slope belongs to the Sesia-Lanzo zone. The area is characterized by pre-Quaternary rock units of the Diorite-kinzigitic complex, gneiss, metagranitoids, metapelites, and eclogitic micaschists (Dal Piaz et al., 1972; Compagnoni et al., 1977; Gosso, 1977; Zucali et al., 2002; Zucali and Spalla, 2011). Quaternary deposits, including banded calcarenite, alluvial and fluvio-glacial sediments, cover parts of the slope and are also involved in the landslide body. The Bosmatto landslide extends for more than 1 km and is mapped as a complex landslide consisting of multiple interacting bodies (fig. 2). The upper portion is imposed on the bedrock of the Eclogitic Micaschists Complex with high-pressure Alpine foliation, while the toe is developed within alluvial and fluvio-glacial deposits. The landslide includes different movements: an upper sector with sliding behaviour and a lateral elongated body extending down to the toe with debris flow characteristics. Two main sectors can be distinguished: a southern inactive, densely vegetated portion, and a northern active portion, without vegetation cover, characterized by large disjointed blocks.

In October 2000, an intense rainfall event caused a sudden reactivation of the landslide, generating a debris flow that mobilized blocks up to 10 m<sup>3</sup>, starting at about 1700 m a.s.l. and channelled into the lateral Letze Creek (Carlà et al., 2019). This event caused several damages to buildings and infrastructures in the Lys Valley. The same event also caused a collapse in the upper portion and the formation of a new scarp above the existing one, around 2100 m a.s.l., as well as additional scarps and tension cracks up to 2300 m a.s.l. in the landslide body. Validation and monitoring have been carried out using a combination of techniques. Carlà et al. (2019) produced a geomorphological map of the Bosmatto landslide, identifying new scarps, fluvial erosion features, and tension cracks. Long-term monitoring with GNSS, satellite InSAR, and GBInSAR over a 16-year period provided quantitative data on the

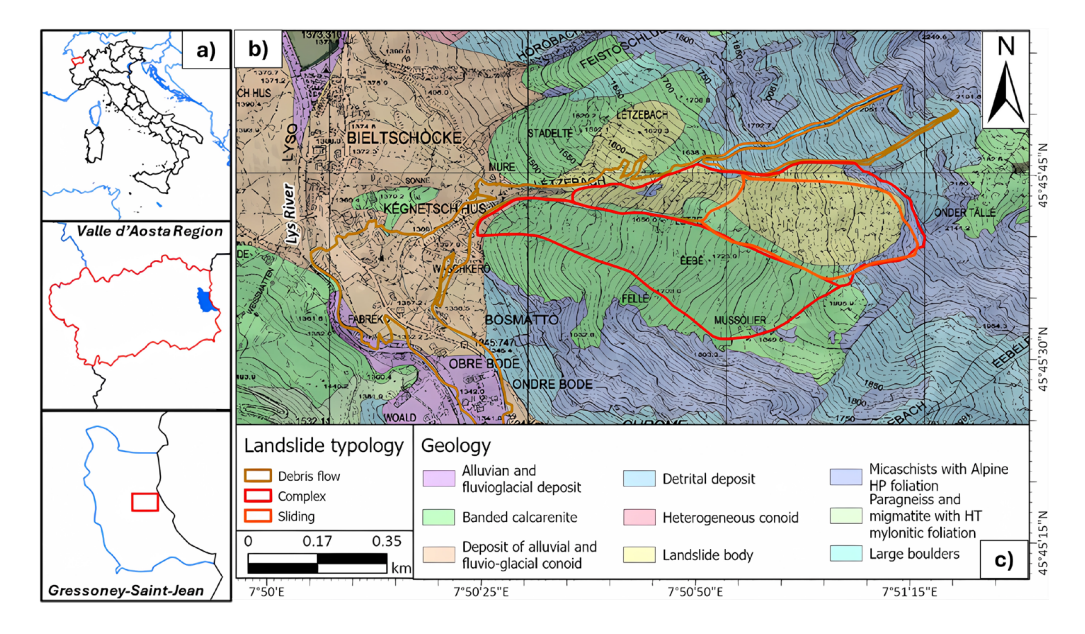


Figure 2 - a) Geographical location of the Bosmatto landslide. b) Geological framework of the Bosmatto landslide in the Valle d'Aosta Region. c) Legend for the geological map of the area.

kinematics, supporting the classification of Bosmatto as a large rockslide with a broadly roto-translational mechanism.

# The Castagnola landslide

The Castagnola landslide is a large landslide with an estimated volume of about 3-6 Mm³, located in the Ligurian Apennines, about 25 km north of La Spezia city and 2.5 km N-NE of the Eastern Ligurian coast. It extends over an area of approximately 0.54 km² (Pazzi *et al.*, 2017). Geologically, the slope belongs to the Inner Ligurian Domain and is characterized by Jurassic to Paleocene oceanic sequences (the "Supergruppo della Val di Vara"), consisting of ophiolites (gabbro, serpentinite, basaltic lavas, ophiolitic breccias) overlain by marine sediments (Monte Alpe Cherts, Calpionelle Limestone, Palombini Shales) of Callovian-Santonian age (Principi *et al.*, 2004, fig. 3). The contrasting lithologies strongly influence slope morphology and stability.

From a geomorphological perspective, the slope shows typical landslide features such as scars and counterslopes, but the morphology is also controlled by the differential erosion of the lithotypes: Palombini Shales correspond to low-relief areas, while serpentinites, gabbros, basalts, and cherts form much steeper slopes. The transition between these morphotypes is sharp and reflects lithological contrasts. Land use mirrors this difference, with settlements and cultivated areas located in the gentler portions and forests on the steepest slopes. The landslide body is bounded to the northeast by a large escarpment and to the southeast by the Rovereto stream, whose erosion enhances slope instability. The landslide mass extends southwest, reaching the right bank of the Castagnola river, diverted by the accumulation of displaced material.

Structurally, the Castagnola landslide is a large complex system characterized by several rotational slips, with shallow planar landslides superimposed. Inclinometer data indicate slip surfaces at depths of 10-20 m in the northern and central sectors, and deeper rotational landslides beyond 20 m at the base of the slope. The displacement rate is on average ~20 mm/year, but with significant spatial variability, making the reconstruction of the overall mechanism challenging (Nosengo, 1987; Pazzi *et al.*, 2017).

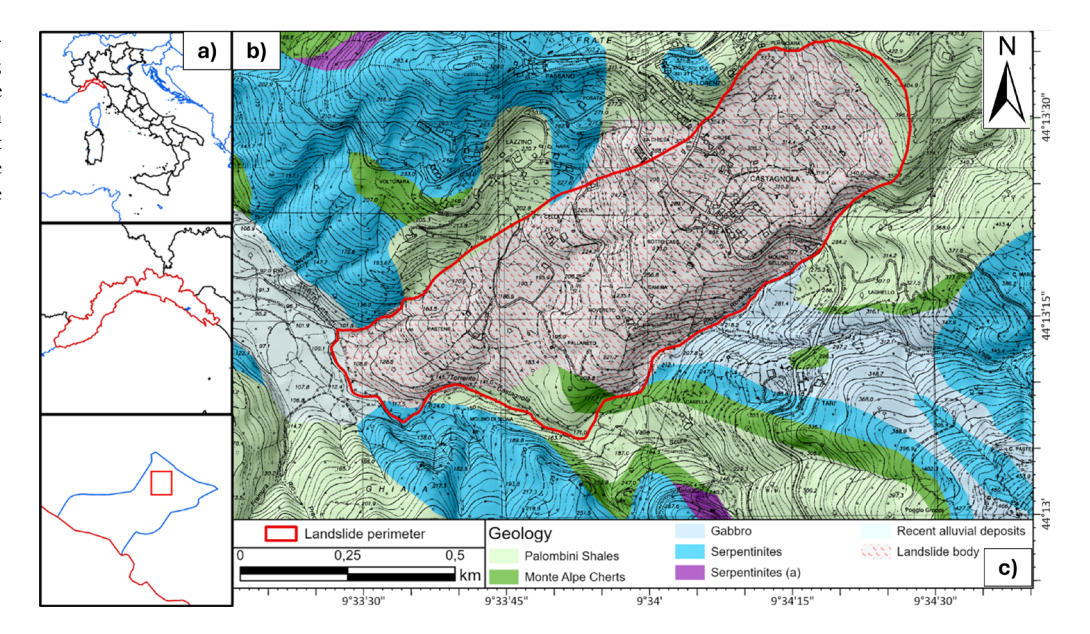
Historically, instability phenomena at Castagnola are well documented. Oral and written sources describe repeated damage to buildings, some of which were abandoned due to recurring slope movements. To this day, lesions attributable to ongoing instability are visible in many houses in Castagnola and the neighbouring hamlets.

Validation and monitoring have been carried out using borehole inclinometers and GBInSAR, which confirmed the presence of multiple slip surfaces and the complex kinematics of the landslide. These results, combined with historical documentation, validate the classification of Castagnola as a large, complex, and still active landslide.

# MATERIALS AND METHODS

Remote sensing technologies, particularly Advanced Differential Interferometric Synthetic Aperture Radar (A-DInSAR), are emerging as powerful tools for mapping the ground deformation processes. The EGMS provides freely available and open-source ground displacement data from the Sentinel-1 satellites, offering a cost-effective solution for wide-scale analysis (Crosetto *et al.*, 2020; Copernicus, 2025; fig. 4).

Figure 3 - a) Geographical location of the Castagnola landslide; b) Geological framework of the Castagnola landslide. From the Regional Geological Chart (CARG) of Liguria region, table 232, modified. c) Legend for the geological map of the area.



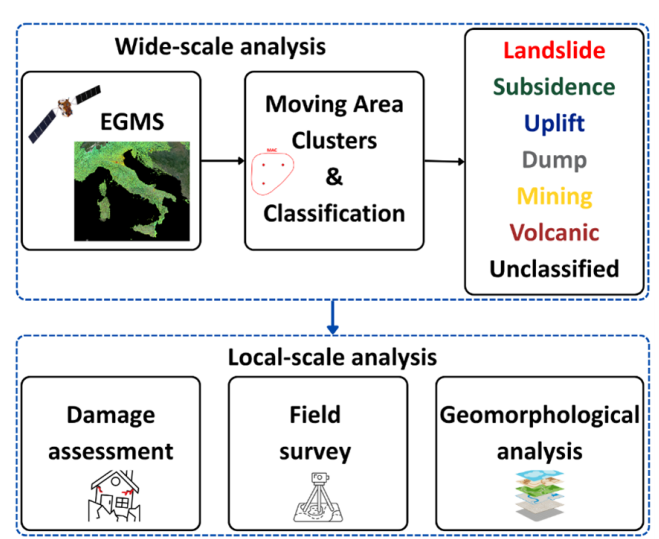


Figure 4 - Flow chart of the adopted methodology for both the wide-scale analysis of the EGMS-InSAR data and the site-specific analysis through field surveys.

Developed within the Copernicus programme, EGMS has been thought and implemented in response to user needs and requirements in the field of ground deformation monitoring. EGMS provides, annually, provides free consistent, reliable and seamless data regarding natural and anthropogenic ground motion over the Copernicus participating states. Products of EGMS consist of InSAR data at three increasing processing levels (Crosetto *et al.*, 2020): i) basic (L2a), ii) GNSS-calibrated (L2b), and iii) Ortho (L3). The L2a basic data deliver Line of sight velocity maps and displacement time series in ascending and descending orbits. L2a basic products are referred to a local reference point. The L2b data are an advanced product, offering absolute deformation maps thanks to the combination of L2a basic data with model derived from global navigation sat-

ellite systems data. Finally, the L3 Ortho products provide vertical and horizontal (east-west) velocity components derived from the L2b data (i.e., still anchored to the reference model used above) resampled on a regular grid with a resolution of 100 m. The horizontal and vertical components of ground motion across the Italian territory were extracted from the EGMS L3 products and subsequently processed using the open-access EGMStream web application (Becattini *et al.*, 2025), which enables rapid download and conversion of the original datasets.

With almost eight million points for each component of deformation, these maps include information that can be exploited to scan wide areas, flag unstable zones and, thanks to the availability of displacement time series, reconstruct the deformation histories of observed areas back to 2019 (fig. 5). Given the enormous availability of InSAR data released regularly, value-added solutions and tools that can optimize data usage are of paramount importance. In general, within the community of non-expert users, there is a need to aggregate and transform InSAR data into usable and operational information.

The aim of this study is to exploit the full potential of the EGMS horizontal and vertical components to support the interpretation of active geological processes throughout the entire Italian territory, a country exposed to a large number of natural hazards, including landslides, subsidence, volcanic eruptions, and earthquakes. In recent years, the major challenge in A-DInSAR analysis has been the management and interpretation of the enormous volume of currently available data, particularly in the context of large and geologically complex regions. The manual characterization of ground deformation areas is a time-consuming task. To address this challenge, an automatic procedure has been developed for the management and analysis of A-DInSAR data, referred to the procedure proposed in Festa *et al.* (2022).

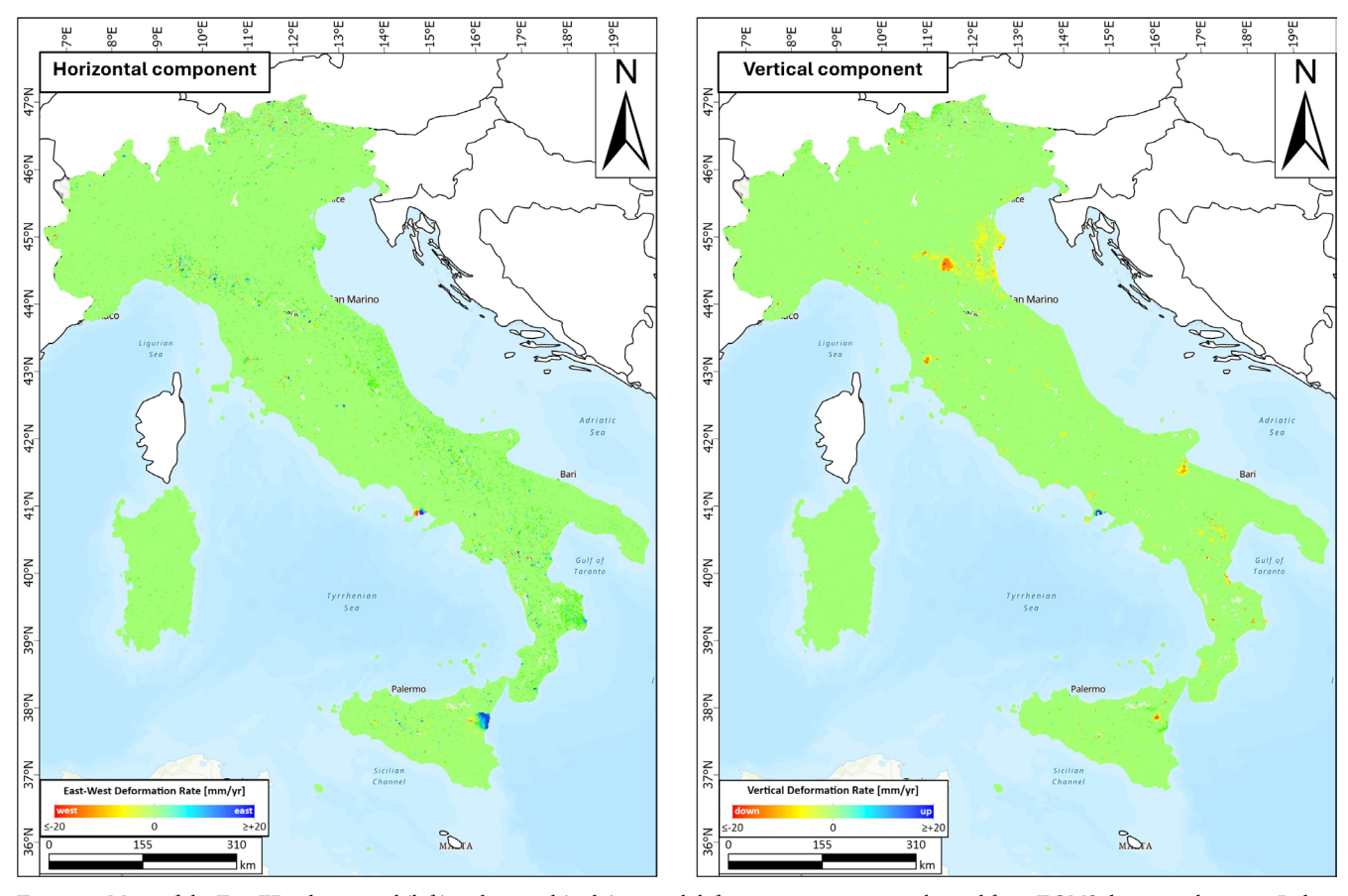


Figure 5 - Maps of the East-West horizontal (left) and vertical (right) ground deformation components derived from EGMS data over the entire Italian territory. The deformation rates are expressed in mm/year and refer to the 2019-2023 period.

This procedure is designed to identify active Measurements Points (MPs) and to aggregate them into polygonal clusters, defined as Moving Area Clusters (MAC). The subsequent classification of these MACs is achieved through the inference of the predominant motion triggering, by the utilization of national homogeneous freely available ancillary data and existing geo-hazard inventory maps. The developed procedure requires three parameters: i) the displacement rate threshold, whose function is to filter out stable MPs; ii) the buffer size, which is the MP radius of "influence" that should be set in accordance with the spatial resolution of the DInSAR dataset (i.e., in this case 100 m); and iii) minimum cluster size, which is referred to the statistically relevant minimum number of MPs to perform spatial clustering. Two velocity thresholds were adopted (±5 mm/year and ±10 mm/year) in order to test their influence on the detection and classification of MACs. The choice of these thresholds is consistent with values commonly adopted in previous InSAR and EGMS-based studies to discriminate significant ground deformation from background noise (e.g., Barra et al., 2017; Navarro et al., 2020; Medici et al., 2025). The ±5 mm/year threshold is suitable for detecting subtle deformation signals, while the  $\pm 10$  mm/year threshold highlights the most active and hazardous processes. Similarly, the buffer size (100 m) was set according to the spatial resolution of the EGMS Ortho products, while the minimum cluster size was chosen following the criteria proposed by Festa et al. (2022) and further optimized through preliminary tests on the Italian dataset. These parameters ensure a balance between capturing real deformation signals and avoiding excessive fragmentation of the results. The resulting MACs have subsequently been classified into ten different categories of both natural and anthropogenic origin through the utilization of a variety of inventories, that are continuous, freely accessible, and homogeneous at the national scale. Specifically, the digital terrain model with a resolution scale of 10 meters (Tarquini and Nannipieri, 2017), the Inventory of Landslide Phenomena in Italy (IFFI) (Trigila et al., 2007), as well as the CORINE Land Cover product (Büttner et al., 2004). The classification of the MACs results as follows: i) landslide, ii) potential landslide, iii) subsidence, iv) potential subsidence, v) dump, vi) mining, vii) deformation related to volcanic, viii) uplift, ix) potential uplift and x) unclassified. The partial or total absence of sufficient input data for the aforementioned model results in an 'uncertain' (as in the case of potential landslides and potential subsidence) or missing (as in the case of the unclassified category) classification of deformation clusters.

Consequently, the present study has led to the identification of susceptible areas of interest that will require further investigation and field surveys. The activities conducted involved the assessment of landslide-induced damage to buildings by applying the approach proposed by Del Soldato *et al.* (2017), which does not necessitate the inspection of structure foundations or interiors.

The cracks and fractures observed in both structures (buildings) and infrastructures (roads) can be grouped into six different categories based on their characteristics and impact on structural integrity:

- No damage, undamaged building;
- ii) Negligible, isolated cracks with a width lower than 1 mm;
- iii) Weak, distortion of the structure not involving the stability and cracks with a width lower than 5 mm;
- iv) Moderate, open cracks that influence the strength of the structure, with width lower than 15 mm;
- v) Severe, spread cracks and fractures, with width lower than 25 mm; and
- vi) Very severe, partial collapse of floors and open cracks, with width greater than 25 mm, which affect structural elements.

The classification of damage was conducted in two phases. The first consisted of a detailed field survey, carried out in March 2025 in the village of Castagnola (Framura, eastern Liguria), where 62 buildings were observed and documented using photographs and damage assessment forms compiled on-site. Each structure was evaluated based on the visible deformation patterns, and classified according to the six levels of damage listed above.

In the second phase, following the matrix proposed by Del Soldato *et al.* (2017), each building was conceptually divided into three sectors to assess the spatial extent of the damage. Based on this evaluation, and using the scoring

matrix provided in Table 3 of the original methodology, each structure was assigned to one of the following eight final damage classes (see also Del Soldato *et al.*, 2019):

- i) No damage;
- ii) Negligible;
- iii) Weak;
- iv) Moderate;
- v) Serious;
- vi) Very serious;
- vii) Potential collapse; and
- viii) Unusable.

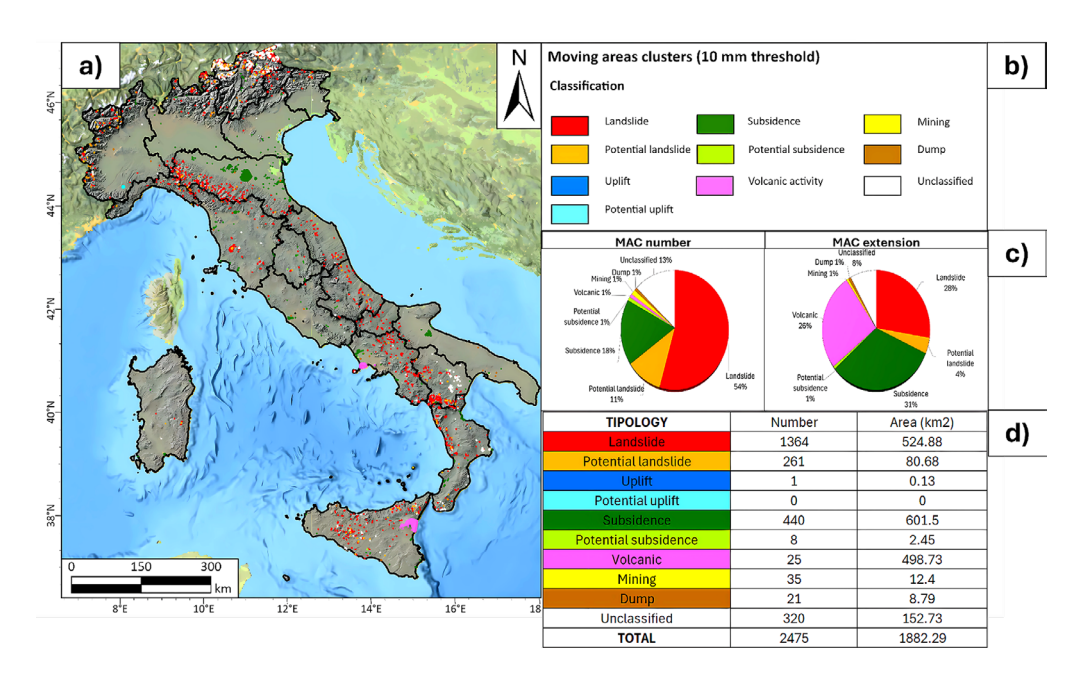
The information collected was georeferenced and processed in ArcGIS Pro to produce a damage map, which delineates the spatial distribution of the observed damage to buildings and, to a limited extent, to access roads and surrounding infrastructure.

#### **RESULTS**

National scale

The analysis of deformation clusters (MAC – Moving Area Clusters) was initially carried out at national scale using EGMS ORTHO data and setting a displacement rate threshold of ±10 mm/year. With this value, a total of 2,475 MACs were identified across the Italian territory, covering a total surface of approximately 1,882 km² (fig. 6). Each cluster was classified according to the predominant deformation process, grouped into natural causes (landslides, subsidence, volcanic activity, uplift) and anthropogenic factors (mining activities, landfills), along with "potential" classes for less-defined phenomena and an "unclassified" category for those not assignable to a specific process.

Figure 6 - Distribution of Moving Area Clusters (MACs) identified across Italy using EGMS data with a ±10 mm/year velocity threshold. Clusters are classified by dominant deformation type. The map highlights the prevalence of landslides and the areal dominance of subsidence and volcanic-related processes. a) Spatial distribution of MACs across Italy with a ±10 mm/year velocity threshold. b) Classification legend of deformation types. c) Pie charts showing the relative number and areal extent of each MAC class. d) Summary table reporting the number and total area of MACs for each typology.



Among the different typologies, landslides emerged as the most frequent, accounting for 54% of all MACs. They were followed by subsidence (18%) and unclassified cases (13%), while the remaining categories appeared with lower frequency. However, in terms of spatial extent, subsidence and volcanic activity assume a higher importance, affecting 31% and 26% of the total area, respectively, compared to 28% for landslides. Interestingly, despite their limited number, volcanic-related deformations – mainly concentrated in the Etna and Campi Flegrei areas – covered extensive surfaces. In contrast, landslides, though more numerous and widespread, tended to be smaller in size and were primarily distributed along the Apennine chain, especially in its northern and southern sectors.

Subsequently, a more sensitive threshold of ±5 mm/year was applied to capture even less pronounced but potentially significant deformation signals (fig. 7). This approach led to the identification of 9,818 MACs, nearly four times the number obtained with the 10 mm/year threshold. The total area affected also increased substantially, reaching 7,335 km², which is approximately a 290% increase. Landslides remained the most represented class in terms of number (40%), followed by subsidence (31%) and unclassified clusters (21%).

From a spatial perspective, subsidence became the dominant typology in terms of area, affecting 46% of the total deformation extent, followed by landslides (28%) and volcanic activity (12%). Once again, volcanic processes, though representing only 1% of the clusters, covered a large portion of the deformed area, confirming their strong areal impact compared to their limited occurrence.

Within the automatic procedure adopted for the classification of ground motion. slope is a key geomorphological parameter for distinguishing between different types of

surface deformation processes. The boxplot in fig. 8 clearly shows that the *Landslide* and *Potential landslide* classes are associated with significantly higher slope values compared to subsidence-related phenomena.

Active landslides show a median slope around 15°, with an interquartile range extending well above 30°, reflecting the typical instability of steep slopes. Potential landslides exhibit a similar behaviour, although with slightly more variability and some cases on gentler slopes, consistent with incipient or latent instability.

On the other hand, the Subsidence and Potential subsidence classes are clearly concentrated at very low slope values, with means and medians well below 5°. This is consistent with the vertical, diffuse nature of subsidence processes, which are commonly associated with flat areas or very gently sloping terrains, such as alluvial plains, coastal zones, or areas affected by groundwater withdrawal or anthropogenic excavations.

The K parameter, defined as the absolute ratio between the vertical and horizontal components of velocity (expressed in cm/year), provides a compact measure of the dominant deformation direction within each MAC.

The boxplot in fig. 9 shows that subsidence clusters are characterized by very high K values, most of them reaching the upper limit (clipped at 15), confirming a strong dominance of vertical motion. *Potential subsidence* clusters follow a similar trend, though with slightly lower values.

In contrast, active landslides show lower K values, typically between 0.3 and 1, indicating a dominant horizontal component, consistent with mass movement along inclined surfaces. *Potential landslides* display a wider distribution of K values, possibly reflecting early-stage deformation where the movement direction has not yet stabilized.

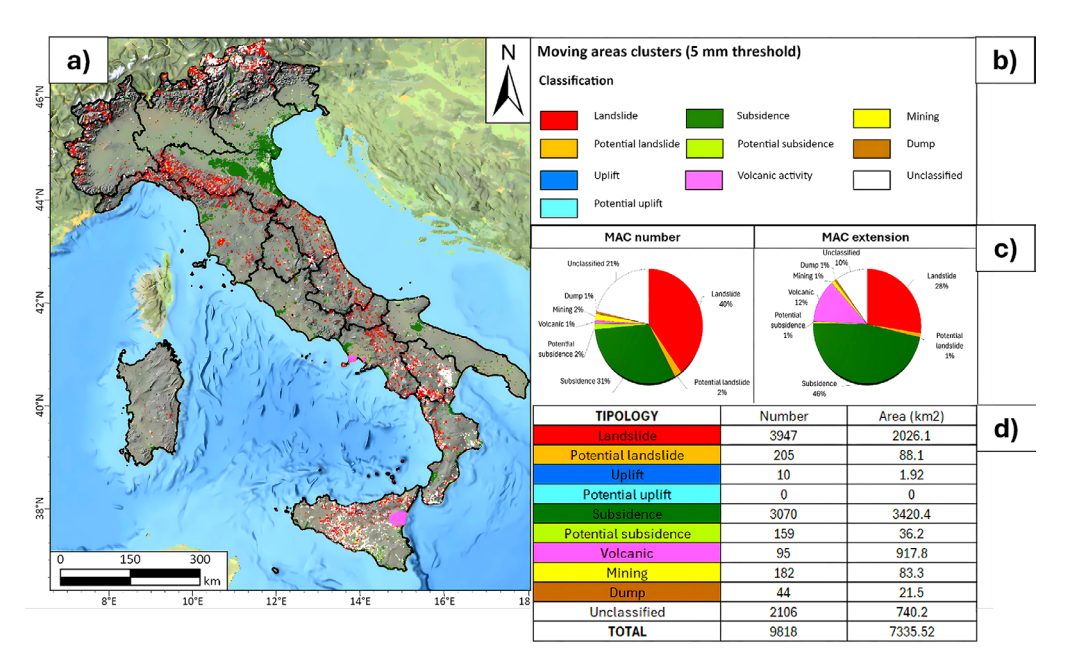


Figure 7 - Distribution of Moving Area Clusters (MACs) detected with a ±5 mm/year velocity threshold. The increased sensitivity allows for the identification of a larger number of deformation clusters, including early-stage or ambiguous signals, particularly in vulnerable areas. a) Spatial distribution of MACs across Italy with a ±5 mm/year velocity threshold. b) Classification legend of deformation types. c) Pie charts showing the relative number and areal extent of each MAC class. d) Summary table reporting the number and total area of MACs for each typology.

When lowering the velocity threshold to 5 mm/year, the same general trends remain evident, but with greater internal variability across all deformation classes. In the case of slope (fig. 10), the distinction between landslide- and subsidence-related clusters remains robust: Landslides and Potential landslides occur on significantly steeper terrain than Subsidence and Potential subsidence. However, the lower threshold includes a broader range of potentially unstable areas, leading to a wider spread in slope values, especially for Potential landslides, some of which are located on surprisingly gentle slopes (i.e., less than 10° in same cases).

Similarly, the distribution of the K parameter (fig. 11) continues to reflect the vertical-horizontal dichotomy of deformation processes, with Subsidence clusters maintaining high K values and Landslides exhibiting lower ones. Yet, the 5 mm dataset also reveals a greater spread in K values, especially for Potential landslides, which may now include clusters with less clear deformation patterns or mixed vertical-horizontal behaviours. This increased vari-

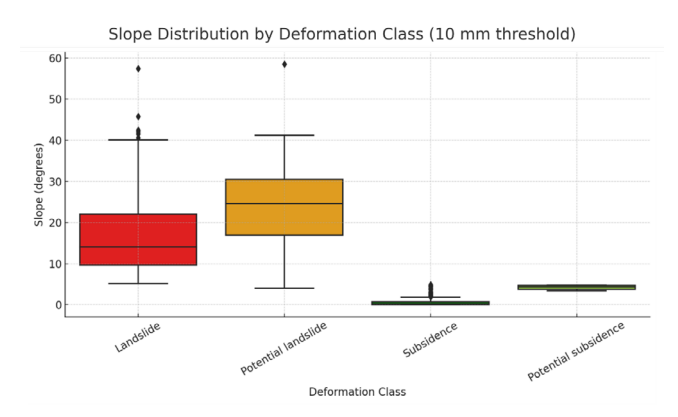


Figure 8 - Boxplot showing the distribution of slope values across different MAC classes using the  $\pm 10$  mm/year threshold. Landslide-related clusters are typically associated with steeper slopes, while subsidence processes occur in flatter areas.

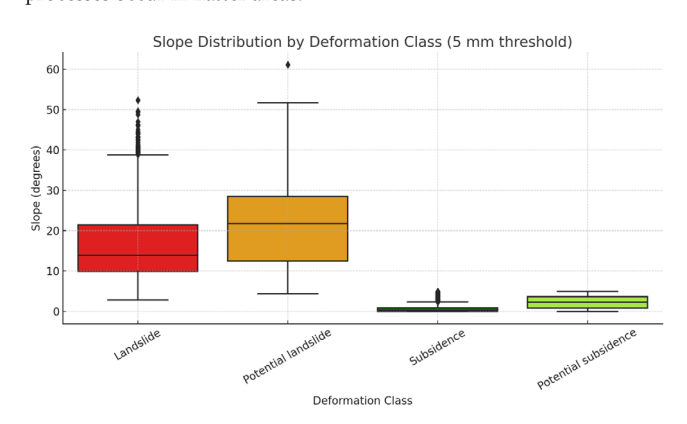


Figure 10 - Slope distribution across MAC classes using the more sensitive  $\pm 5$  mm/year threshold. The wider spread of slope values for Potential landslides reflects the inclusion of incipient or low-magnitude movements.

ability is consistent with the inclusion of slower and potentially more ambiguous deformation processes when using a more sensitive threshold.

Benefitting the enhanced imaging capabilities of Sentinel-1 and leveraging on the proposed approach, based on the spatial filtering, clustering and classification of ground deformation maps it has been possible to screen wide areas, spot active movements and flag instabilities events. Following the identification, at national scale, of unstable zones, it is possible to shortlist instabilities events. This means that prioritisation and mitigation strategies for risk reduction can start at local scale, with satellite radar data and prioritise those instabilities that represent a major threat and are deemed to be most urgent.

Outcomes of the proposed procedure at national scale allowed pinpointing unstable areas related to slope instabilities across the Italian territory and can be adopted as key layers for further analysis. In the next paragraph two examples are reported, the Bosmatto and the Castagnola landslide in the Alpine and Apennines chain, respectively.

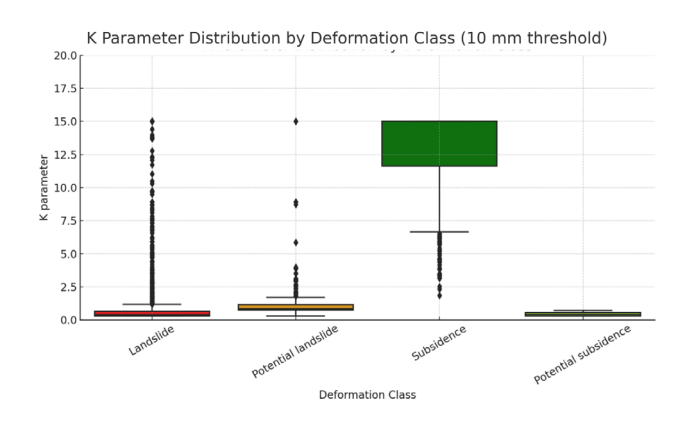


Figure 9 - Boxplot of the K parameter (ratio between vertical and horizontal velocity components) for the  $\pm 10$  mm/year threshold. High K values indicate vertically dominated motion typical of subsidence, while landslides show lower values due to horizontal displacement.

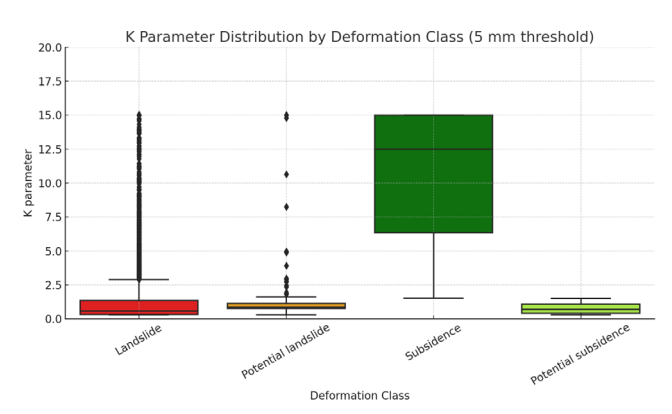


Figure 11 - Distribution of K parameter for MACs identified with the  $\pm 5$  mm/year threshold. The increase in variability, especially in Potential landslides, reflects the detection of less clear or mixed deformation patterns.

# Bosmatto landslide InSAR monitoring

The L3 EGMS data, thus the horizontal East-West and the vertical component of the velocity, over the Bosmatto landslide has a low, but meaningful, coverage of data. In fact, over the mapped landslide only eight MPs in the upper portion are present due to the dense vegetation coverage. The horizontal component (fig. 12a) show negative velocities (from -6 mm/year up to -20.8 mm/year), this indicating a Westward movement, and a cumulative displacement from 15.1 mm and 113.3 m, respectively, from January 2019 to December 2023. The sample time-series, referring to the point characterized by the higher velocity, show from 2019 to the end of 2023 a linear trend with a slightly deceleration from the spring/summer 2023. The vertical component deformation map (fig. 12b) exhibits negative values, referring to down movement with annual velocity from -4.0 mm/year up to -17.0 mm/year with a cumulative displacement of 11.6 mm and 78.2 mm, respectively, in five years of analysis. The sample time-series of the fastest point confirms no relevant acceleration or deceleration and a low decelerating trends, mainly from the beginning of 2023.

The availability of the E-W and vertical components gives the opportunity to estimate the true movement vector, having in mind that the horizontal component is underestimated since N-S movements cannot be extracted with current satellite platforms. Nonetheless, the calculated easting component will provide an almost truthful es-

timation of the horizontal component in the case of nearly E-W planimetric movements of the slope, such as the Bosmatto landslide.

It is possible to derive the approximated angle of dip (as a ratio of E-W to vertical velocity), whose variation along the slope indicates which is the predominant component. Not surprisingly, for the Bosmatto landslide the horizontal component progressively becomes more predominant from head to toe.

In the head scarp area vertical component is predominant, then gradually the movement becomes sub-parallel to the slope surface, and ultimately the velocity vector slightly dips out of the slope in proximity of the toe.

Based on the analysis of the monitoring data, Carlà *et al.* (2019) inferred that the Bosmatto landslide is a large rockslide that also involves deformation of the bedrock at depth. The gradual rotation of the dip angles of movement indicates that the instability evolves according to a broadly roto-translational mechanism.

# Castagnola landslide InSAR monitoring

The interferometric data of L2b EGMS over the slope affected by the landslide in Castagnola refer to one track in ascending orbit and two tracks in descending orbit. The data of the horizontal east-west and vertical velocity components have too coarse spatial sampling and were therefore not considered for the analyses presented in

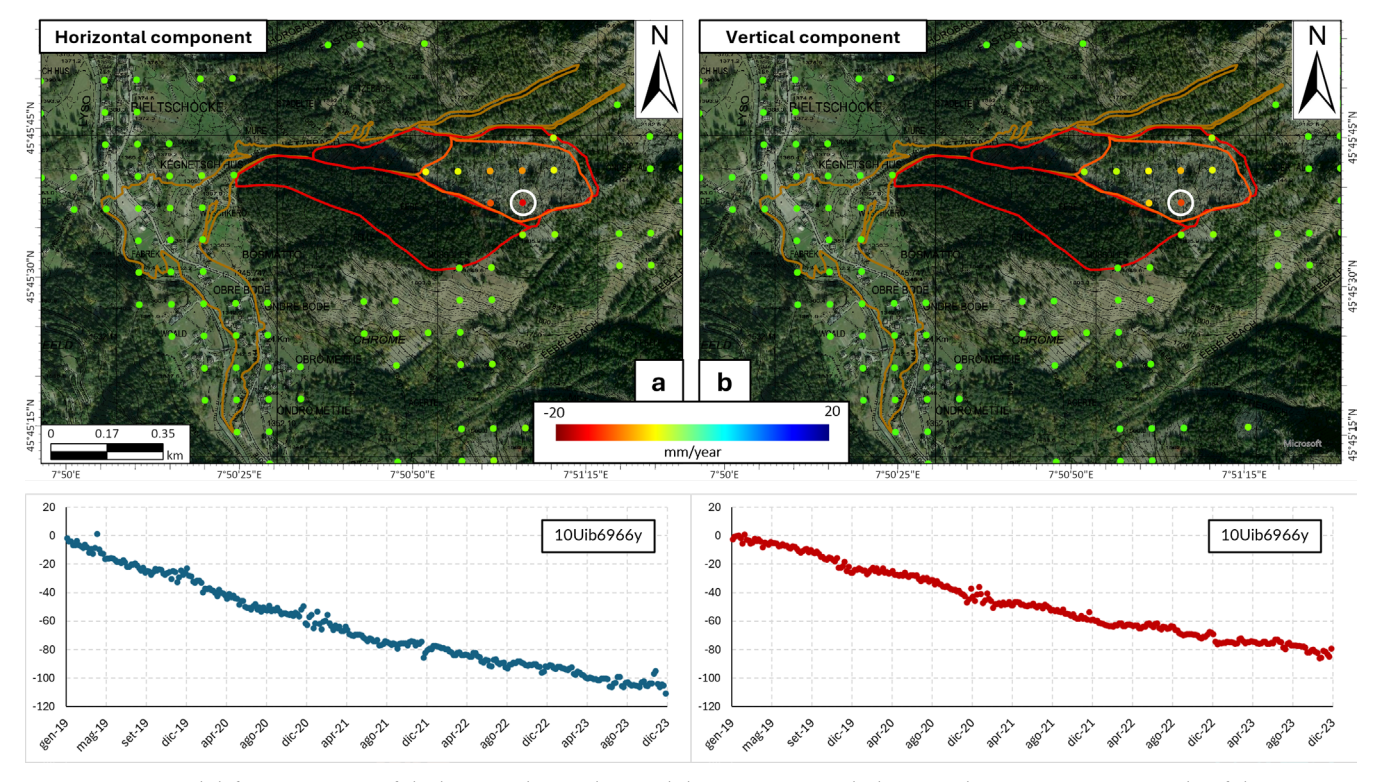


Figure 12 - Ground deformation maps of the horizontal (a) and vertical (b) component. with their sample time-series, respectively, of the L3 EGMS data over the Bosmatto landslide.

this paper. The data, both in ascending and descending geometry, show good coverage over the village of Castagnola, which is in an intermediate position with respect to the general extent of the landslide. In particular, the data acquired in the ascending orbit seem to be better distributed than those acquired in the descending orbit, showing points also in the areas at lower elevation. No radar targets are available in the upper part, which includes the main ridge of the landslide, given the dense vegetation cover and the lack of reflective object which limit the imaging capabilities of the C-band used by Sentinel-1 satellites.

Overall, the velocities that characterized the 5 years of observation, measured along the LOS of the sensor, show average values between 11 mm/year and 24 mm/year in ascending orbit, with cumulative displacements of up to 120 mm (fig. 12a) and between -38 mm/year and 51 mm/year in descending orbit, with cumulative displacements of up to 220 mm (fig. 12b).

The sign discordance of the values measured in the two orbital configurations (positive for the ascending geometry and negative for the descending geometry) indicates a strong horizontal component of the measured movement. In this case, the slope aspect suggests a general component of movement directed toward the southwest, which allows for a good estimate of the movement in the data acquired both in ascending geometry and, albeit to a lesser extent, in descending geometry.

The time series shown in fig. 13 show trends characterized by weak seasonality, i.e. phases of slight acceleration in the late winter and spring months and deceleration in the summer months. Both displacement time-series show a slight slowdown from spring 2023 to the end of the observation period (December 2023), a period characterized by a lack of precipitation.

This fact testifies to the reliability of the available data, which are able to detet even small variations in the landslide behaviour due to variations in the triggering factors, such as rainfall and the related fluctuations in the groundwater level.

In parallel with the interferometric analysis, a field-based damage assessment survey was conducted in March 2025 in the village of Castagnola, with the aim of evaluating the impact of the landslide on the built environment. The adopted methodology follows the two-step procedure proposed by Del Soldato *et al.* (2017), which allows for a rapid and systematic classification of damage to buildings based solely on observable surface features, without the need for internal inspection.

A total of 62 buildings were surveyed, each one photographed and assessed using standardized forms. The visible structural damage was initially classified into six severity levels (from No damage to Very severe), and then, based on the areal extent of the observed damage, each structure was assigned to one of the eight final damage classes defined by the methodology (Table 3 in Del Soldato *et al.*, 2017).

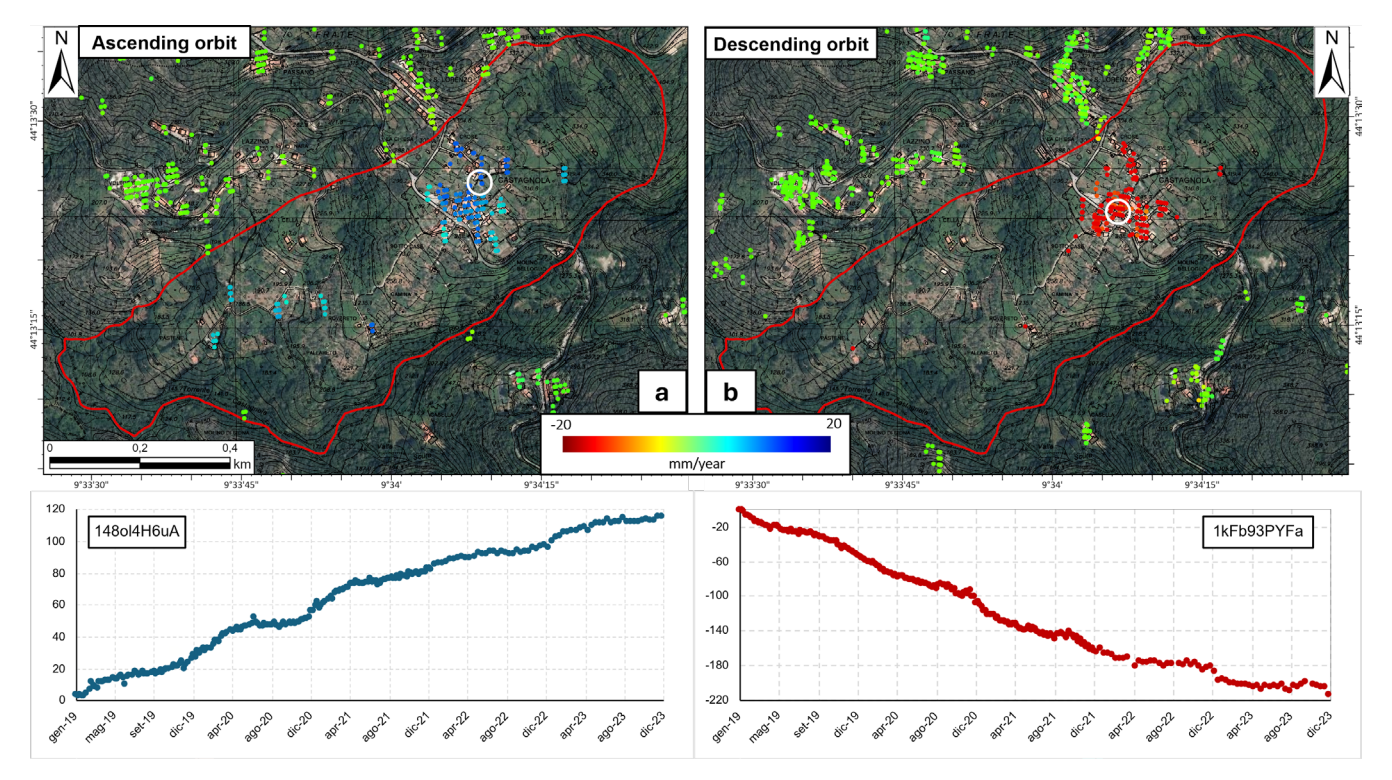


Figure 13 - Ground deformation maps obtained using data acquired in ascending (a) and descending (b) orbit, with their sample time-series, respectively, of the L3 EGMS data over the Castagnola landslide. The IDs of the points associated with the time series are specified on the graph areas.

The resulting damage distribution shows that the majority of buildings exhibit limited to moderate damage:

- No damage: 1 building;Weak: 24 buildings;
- Negligible: 13 buildings;
- Serious: 8 buildings;
- Very serious: 3 buildings;
- Potential collapse: 1 building;
- Unusable: 1 building.

The mapped distribution of these classes highlights a spatial correlation between the interferometric displacement patterns and the severity of structural damage, with the most affected buildings located in the lower part of the village, where deformation is more evident. The collected field data complement the satellite-based observations and provide a more comprehensive picture of the current state of instability and its impact on the urban fabric.

The mapped results are illustrated in fig. 14, which shows the spatial distribution of buildings in Castagnola according to the assigned damage class. The most severe damage levels (Very serious, Unusable, and Potential col-

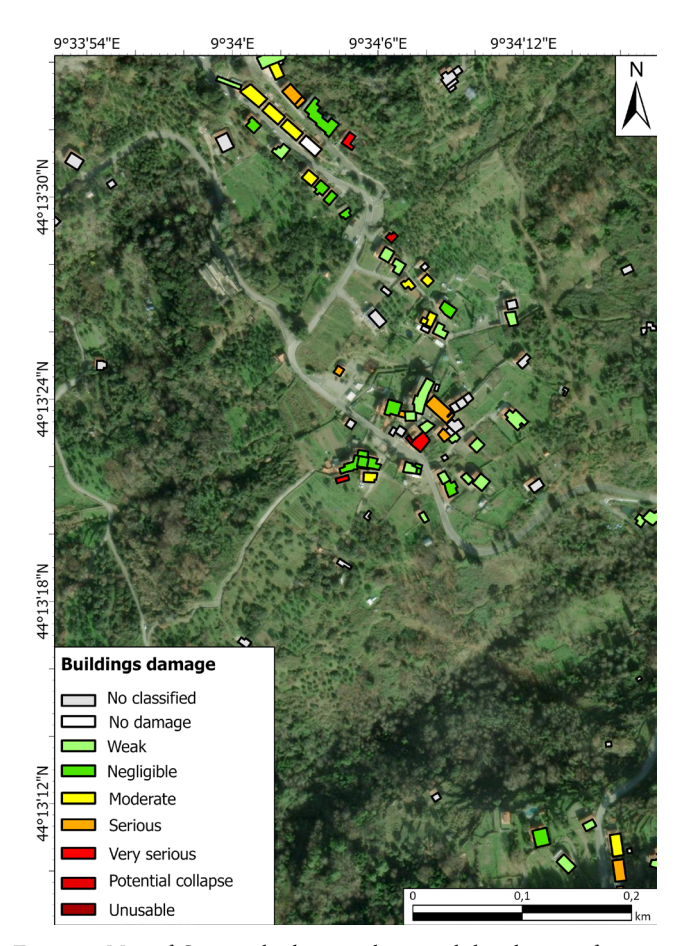


Figure 14 Map of Castagnola showing the spatial distribution of structural damage classes assigned to the 62 surveyed buildings, based on the methodology of Del Soldato *et al.* (2017). The classification includes eight levels ranging from "No damage" to "Unusable".

lapse) are spatially concentrated in the southwestern sector of the village, in correspondence with higher cumulative displacements observed in the interferometric data.

In addition, fig. 15 presents selected field photographs that document representative examples of structural damage observed during the survey, including severe cracking on walls and roads. These visual elements support the classification and highlight the real-world impact of the ongoing slope instability on the local infrastructure.

## DISCUSSION

The results obtained through the proposed automated classification procedure of Moving Area Clusters (MACs) confirm the significant potential of open-source InSAR data, particularly the EGMS product, for the detection and geomorphological characterization of surface deformation processes at multiple spatial scales. The adopted methodology proved to be robust and adaptable, capable of providing coherent and meaningful outputs both at the national level and in complex local settings.

The national-scale analysis clearly demonstrates how the choice of displacement velocity threshold influences not only the number of detected clusters but also their nature, geographical distribution, and classification. The more conservative threshold of ±10 mm/year led to the identification of 2,475 MACs, representing the most intense and easily interpretable deformations. In this context, landslides were the most frequent process in terms of number of clusters, while subsidence dominated in terms of affected surface area, particularly across the large alluvial plains of northern Italy. The distinction between these two processes is also clearly reflected in the morpho-kinematic parameters: landslides are typically associated with higher slope values and lower K values, indicating a dominant horizontal movement component, whereas subsidence occurs in areas of very low slope and high K values, reflecting primarily vertical motion. These results validate the approach and highlight how the integration of geometric and kinematic parameters can significantly enhance the automatic classification of deformation types.

The application of a more sensitive ±5 mm/year threshold, aimed at maximizing detection capability, led to the identification of over 9,800 MACs – nearly four times more than with the higher threshold. This increase also resulted in greater interpretative complexity, with a significant growth in "potential" and "unclassified" clusters. Such behaviour was expected and reflects the inclusion of weaker or early-stage deformation signals, which may not be immediately critical but whose early detection is important because potentially relevant for long-term monitoring. These signals are not randomly distributed but often cluster in vulnerable areas, either known to be unstable or under anthropogenic pressure.



Figure 15 Examples of damage observed during the March 2025 field survey in Castagnola. The photographs show: a) staircase partially detached from the structure; b) deep wall cracks; c) diagonal crack on a multi-storey building; d) longitudinal cracks affecting road pavement. These cases fall within the Serious to Very Serious categories.

An important aspect concerns the presence of "potential" and "unclassified" categories within the classification outputs. These groups account for a non-negligible proportion of the total MACs and represent areas where the available ancillary information was insufficient to support a confident interpretation. Potential landslides and potential subsidence clusters typically correspond to deformation signals consistent with the expected process but not confirmed by national inventories (e.g., IFFI, land use maps). The unclassified clusters, on the other hand, mainly occur in urbanized or geologically complex areas, where deformation signals cannot be reliably attributed to a specific process. The existence of these categories poses some challenges: they may reduce operational efficiency and, if misinterpreted, could generate false positives in hazard mapping. Nevertheless, they also play an important conservative role, as they prevent forcing unreliable classifications and instead isolate ambiguous signals that can be prioritized for further field validation or integration with complementary datasets. In this way, uncertain categories highlight areas of potential interest without compromising the robustness of the national-scale analysis.

The comparison between the two thresholds confirms that the ±10 mm/year threshold is more suitable for operational purposes, offering clearer classification and reduced signal ambiguity. Conversely, the ±5 mm/year threshold is

more appropriate for early warning and pre-screening strategies, as it allows for the detection of weak anomalies that may evolve into more hazardous processes over time. In this sense, adopting a multi-threshold approach supported by automated classification offers an effective solution for balancing precision and sensitivity, enhancing the responsiveness of monitoring systems across multiple scales.

This dual-scale approach offers a flexible framework that can be adapted to the needs of various end users, ranging from local authorities requiring precise, actionable insights to national agencies focused on broader-scale monitoring and prioritization. The final output of this analysis is a geodatabase of areas characterized by active motions that can be used users and authorities in multiple ways, from updating geo-hazard inventories, to prioritization of intervention /starting from situations most urgent) and to planning effectively local risk reduction actions.

The application of the methodology at the local scale allowed for a more detailed assessment of its effectiveness in two highly different case studies: the Bosmatto landslide in Valle d'Aosta Region and the Castagnola landslide in Liguria Region. These two sites differ significantly in terms of lithology, morphology, deformation style, and anthropogenic interference.

In the Bosmatto case, the landslide is located in a mountainous area with complex alpine topography, dense vegetation, and slow movement. Despite limited point density, EGMS data revealed coherent displacement patterns, with LOS velocities ranging from -4 to -20 mm/year and no significant accelerations during the observation period. Although the radar geometry and vegetation cover limit the extent of measurement points, the EGMS product proved capable of detecting ongoing deformation in forested areas and providing objective, long-term temporal insights. The Bosmatto landslide is also a perfect example on how satellite interferometry can contribute to the detection and characterization of the affected area, complementing the existing ground-based monitoring system and supporting the interpretation of the landslide mechanism.

By contrast, the Castagnola landslide, located in a densely built-up hilly area, showed greater spatial coverage, with high point density and well-distributed signals. LOS velocities reached ±11 to ±38 mm/year, with cumulative displacements exceeding 200 mm. The combination of ascending and descending orbits revealed a predominantly horizontal movement component, consistent with the slope aspect and the known landslide dynamics. Additionally, the time series analysis detected seasonal oscillations in the signals – likely related to rainfall patterns – as well as a slight deceleration in 2023, suggesting sensitivity of the EGMS product to environmental triggers and hydrogeological changes.

In addition to the interferometric analyses, the damage survey conducted in Castagnola in March 2025 allowed a direct validation of the deformation signals using groundbased evidence. The documented structural damage, which includes a wide spectrum of severity levels – from negligible cracks to potential collapse – further supports the interferometric findings, confirming the ongoing impact of the landslide on the built environment. The spatial distribution of damage classes correlates well with the interferometric displacement data, especially in the southwestern sector of the village where the highest deformation rates were recorded. This integrated analysis highlights the added value of combining EGMS data with systematic field-based damage assessments. The approach not only enhances the reliability of satellite-derived information but also enables a more complete characterization of hazard scenarios at the local scale. As such, the Castagnola case demonstrates the operational relevance of coupling interferometric monitoring with in situ damage evaluation for risk assessment, particularly in densely populated or historically affected areas.

These findings demonstrate that the proposed approach, supported by open-access EGMS data, can adapt to diverse geomorphological and anthropogenic settings, providing reliable outputs even in the presence of noise and external disturbances. The integration between national-scale mapping and local-scale validation reinforces the versatility of the method and highlights its potential applicability in other European or global contexts.

The main strength of the proposed procedure lies in its high level of automation, which enables rapid extraction and classification of deformation phenomena over large areas and makes the approach replicable in other settings. Furthermore, the integration of morphometric and kinematic parameters helps reduce the subjectivity typically associated with manual interpretation, improving the objectivity and reproducibility of the results.

However, some limitations remain. These include the dependence on point density (affected by land cover and satellite acquisition geometry), and classification ambiguity in marginal cases, which tends to increase when using lower thresholds. These aspects highlight the importance of integrating ancillary data (e.g., field surveys, geological maps, thematic inventories) to refine interpretations, especially in complex or borderline situations.

Future improvements may include the incorporation of machine learning classifiers, context-specific dynamic thresholds, and synergy with complementary geospatial datasets such as GNSS, LiDAR, and UAV-based observations. Additionally, the use of thematic geodatabases (*e.g.*, landslide inventories, geological maps, land use layers) could significantly improve classification accuracy and operational relevance, paving the way for a replicable, updatable and scalable deformation monitoring system to support land management and hazard mitigation policies.

# **CONCLUSION**

This work demonstrates the effectiveness and applicability of open-access InSAR data, specifically the European Ground Motion Service (EGMS) products, in the detection and geomorphological classification of surface deformation processes across multiple spatial scales. The implementation of a fully automated processing and classification workflow allowed for the extraction of deformation clusters (MACs) across the entire Italian territory, yielding meaningful and consistent results that highlight both the strengths and the current limitations of using open-source EO data for geomorphological applications.

At the national scale, the proposed methodology proved capable of identifying and classifying over 2,000 deformation clusters using a conservative velocity threshold of ±10 mm/year, and nearly 10,000 using a more inclusive ±5 mm/year threshold. These findings confirm that the velocity threshold plays a critical role in controlling the number, type, and spatial distribution of detected phenomena. The higher threshold is particularly effective in isolating well-defined, intense deformation patterns, such as active landslides and subsidence in major basins, while the lower threshold allows for the inclusion of weaker, more ambiguous deformation signals that may indicate early-stage processes or complex, multi-source dynamics.

The morpho-kinematic analysis confirms the reliability of slope and K parameters in distinguishing between different types of deformation: landslides typically occur on steeper slopes with dominant horizontal movement, while subsidence affects flatter areas and is predominantly vertical. These indicators proved to be valuable tools for the automatic classification and prioritization of deformation phenomena.

The two local case studies, Bosmatto and Castagnola, allowed us to assess the performance of the methodology in contrasting geomorphological settings. In Bosmatto, a slow-moving landslide in a forested mountainous area, the EGMS data showed coherence despite limited point density, confirming the method's robustness even in low-return environments. In Castagnola, located in a densely urbanized hilly sector, the EGMS data revealed high LOS velocities and significant cumulative displacements, capturing both the horizontal component of motion and the seasonal dynamics related to rainfall. These results validate the utility of open InSAR data for detailed site-specific analysis, especially when supported by appropriate interpretation tools and contextual information.

Importantly, the analysis in Castagnola was supported by a detailed field-based damage assessment survey, conducted in March 2025, which provided an independent validation of the InSAR-derived motion patterns. A total of 62 buildings were inspected and classified into eight damage categories following the methodology of Del Soldato et al. (2017), ranging from No damage to Unusable. The results showed that most buildings were moderately to weakly damaged, while a few exhibited serious to very serious structural impairments. The spatial distribution of damage strongly correlates with the mapped deformation signals, reinforcing the reliability of the satellite data and demonstrating the added value of integrating InSAR monitoring with systematic field observations. This case highlights the practical potential of such combined approaches in densely populated and vulnerable areas.

Overall, this study confirms that the integration of open-source InSAR data with automated spatial analysis, clustering algorithms, and geomorphological parameters can support the large-scale mapping and classification of surface deformation. The approach is replicable, scalable, and adaptable, making it suitable for implementation in other countries and for other ground motion phenomena.

Nevertheless, some limitations must be acknowledged. The density and quality of EGMS measurement points are strongly influenced by land cover, with forested, snow-covered, and agricultural areas often characterized by sparse or inconsistent data. Urban environments may introduce decorrelation or noise linked to building materials and infrastructure, while steep slopes not oriented towards the radar line-of-sight can reduce data coverage. These factors may lead to incomplete detection or ambiguous classifi-

cation of clusters, particularly when using lower velocity thresholds. Therefore, while the methodology is robust and scalable, its operational applicability is constrained in low-return SAR areas or highly heterogeneous terrains. In these contexts, the integration of complementary datasets (e.g., GNSS, LiDAR, geological and land use maps, or field surveys) is essential to improve classification accuracy and reduce uncertainty.

Future developments should focus on enhancing classification in ambiguous cases – particularly those associated with low-magnitude signals or overlapping deformation processes - through the integration of ancillary datasets (e.g., geological maps, land use, rainfall records) and machine learning-based classification schemes. Moreover, a dynamic weighting system for the classification parameters could improve sensitivity to context-specific deformation behaviours. Ultimately, the methodology presented here contributes to bridging the gap between Earth observation data availability and its practical uptake in geomorphological monitoring and risk mitigation. Ultimately, the methodology presented here contributes to bridging the gap between Earth observation data availability and its practical uptake in geomorphological monitoring and risk mitigation.

#### AUTHOR CONTRIBUTION

Francesco Becattini: Writing - original draft, Visualization, Methodology, Investigation, Data elaboration, Conceptualization. Francesco Poggi: Methodology, Formal analysis, Data elaboration. Luca Tanteri: Writing - original draft, Investigation, Visualization. Pierluigi Confuorto: Writing - original draft, Review and editing, Methodology, Data elaboration, Validation. Matteo Del Soldato: Review and editing, Methodology, Investigation, Data elaboration, Validation. Sandro Moretti: Review and editing, Supervision, Resources. Federico Raspini: Writing - original draft, Review and editing, Validation, Supervision, Conceptualization.

#### **ACKNOWLEDGMENTS**

PhD of Francesco BECATTINI is funded by European Union - Next-GenerationEU - Mission 4 "Education and Research" - Component 2 "From Research to Business" - Investment 3.1 "Fund for the realization of an integrated system of research and innovation infrastructures" - Project IR0000037 - GeoSciences IR - CUP I53C22000800006.

#### REFERENCES

Agliardi F., Zanchi A., Crosta G.B., 2022. Tectonic vs. gravitational morphostructures in the central Eastern Alps (Italy): constraints on the recent evolution of the mountain range. Tectonophysics, 474 (1-2), 250-270. https://doi.org/10.1016/j.tecto.2009.02.019

Barra A., Solari L., Béjar-Pizarro M., Monserrat O., Bianchini S., Herrera G., Moretti S., 2017. *A methodology to detect and update active deformation areas based on Sentinel-1 SAR images*. Remote Sensing, 9, 1002. https://doi.org/10.3390/rs9101002

- Becattini F., Medici C., Festa D., Del Soldato M., 2025. EGMStream Webapp: EGMS Data Downstream Solution. Geosciences, 15, 154. https://doi.org/10.3390/geosciences15040154
- Bianchini S., Cigna F., Righini G., Proietti C., Casagli N., 2012. Landslide hotspot mapping by means of persistent scatterer interferometry. Environmental Earth Sciences, 67, 1155-1172. https://doi.org/10.1007/s12665-012-1559-5
- Busetti A., Calligaris C., Forte E., Areggi G., Mocnik A., Zini L., 2020. Non-invasive methodological approach to detect and characterize highrisk sinkholes in urban cover evaporite karst. Remote Sensing, 12, 3814. https://doi.org/10.3390/rs12223814
- Büttner G., Feranec J., Jaffrain G., Mari L., Maucha G., Soukup T., 2004. *The CORINE land cover 2000 project.* EARSeL eProceedings, 3, 331-346.
- Carlà T., Tofani V., Lombardi L., Raspini F., Bianchini S., Bertolo D., Casagli N., 2019. Combination of GNSS, satellite InSAR, and GBIn-SAR remote sensing monitoring to improve the understanding of a large landslide in high alpine environment. Geomorphology, 335, 62-75. https://doi.org/10.1016/j.geomorph.2019.03.014
- Carminati E., Martinelli G., 2002. Subsidence rates in the Po Plain, northern Italy: the relative impact of natural and anthropogenic causes. Engineering Geology, 66, 241-255. https://doi.org/10.1016/ S0013-7952(02)00031-5
- Compagnoni R., Dal Piaz G.V., Hunziker J.C., Gosso G., Lombardo B., Williams P.F., 1977. The Sesia-Lanzo Zone: a slice of continental crust, with alpine HP-LT assemblages in the Western Italian Alps. Rendiconti della Società Italiana di Mineralogia e Petrologia, 281-334.
- Confuorto P., Casagli N., Casu F., De Luca C., Del Soldato M., Festa D., Lanari R., Manzo M., Onorato G., Raspini F., 2023. Sentinel-1 P-SBAS data for the update of the state of activity of national landslide inventory maps. Landslides, 20, 1083-1097. https://doi.org/10.1007/s10346-022-02024-0
- Copernicus, 2025. European Ground Motion Service.
- Crosetto M., Solari L., Mróz M., Balasis-Levinsen J., Casagli N., Frei M., Oyen A., Moldestad D.A., Bateson L., Guerrieri L., Comerci V., Andersen H.S., 2020. The evolution of wide-area DIn-SAR: from Regional and National Services to the European Ground Motion Service. Remote Sensing, 12, 2043. https://doi.org/10.3390/ rs12122043
- Dal Piaz G.V, Hunziker J.C., Martinotti G., 1972. La Zona Sesia-Lanzo e l'evoluzione tettonico-metamorfica delle Alpi Nordoccidentali interne. Memorie della Società Geologica Italiana, 11, 433-460.
- Del Soldato M., Bianchini S., Calcaterra D., De Vita P., Martire D.D., Tomás R., Casagli N., 2017. A new approach for landslide-induced damage assessment. Geomatics, Natural Hazards and Risk, 8, 1524-1537. https://doi.org/10.1080/19475705.2017.1347896
- Del Soldato M., Farolfi G., Rosi A., Raspini F., Casagli N., 2018. Subsidence evolution of the Firenze-Prato-Pistoia Plain (Central Italy) combining PSI and GNSS Data. Remote Sensing, 10, 1146. https://doi.org/10.3390/rs10071146
- Del Soldato M., Solari L., Poggi F., Raspini F., Tomás R., Fanti R., Casagli N. 2019. Landslide-induced damage probability estimation coupling In-SAR and field survey data by fragility curves. Remote Sensing, 11 (12), 1486. https://doi.org/10.3390/rs11121486
- Doglioni C., 1991. A proposal for the kinematic modelling of W-dipping subductions. Possible applications to the Tyrrhenian-Apennines system. Terra Nova, 3, 423-434. https://doi.org/10.1111/j.1365-3121.1991. tb00172.x

- Eckerstorfer M., Eriksen H.Ø., Rouyet L., Christiansen H.H., Lauknes T.R., Blikra L.H., 2018. Comparison of geomorphological field mapping and 2D-InSAR mapping of periglacial landscape activity at Nordnesfjellet, northern Norway. Earth Surface Processes and Landforms, 43, 2147-2156. https://doi.org/10.1002/esp.4380
- Famiglietti N.A., Miele P., Defilippi M., Cantone A., Riccardi P., Tessari G., Vicari A., 2024. Landslide mapping in Calitri (Southern Italy) using new multi-temporal InSAR algorithms based on permanent and distributed scatterers. Remote Sensing, 16, 1610. https://doi.org/10.3390/rs16091610
- Festa D., Bonano M., Casagli N., Confuorto P., De Luca C., Del Soldato M., Casu F., 2022. Nation-wide mapping and classification of ground deformation phenomena through the spatial clustering of P-SBAS In-SAR measurements: Italy case study. ISPRS Journal of Photogrammetry and Remote Sensing, 189, 1-22. https://doi.org/10.1016/j.isprsiprs.2022.04.022
- Gosso G., 1977. Metamorphic evolution and fold history in the eclogitic micaschists of the upper Gressoney Valley (Sesia-Lanzo Zone, Western Alps). Rendiconti della Società Italiana di Mineralogia e Petrologia, 389-407.
- Gutiérrez F., Galve J.P., Lucha P., Castañeda C., Bonachea J., Guerrero J., 2011. Integrating geomorphological mapping, trenching, InSAR and GPR for the identification and characterization of sinkholes. Geomorphology, 134, 144-156. https://doi.org/10.1016/j.geomorph.2011.01.018
- Hearn G.J., 2019. *Geomorphology in engineering geological mapping and modelling*. Bulletin of Engineering Geology and the Environment, 78, 723-742. https://doi.org/10.1007/s10064-017-1166-5
- Hu Y., Liu L., Huang L., Zhao L., Wu T., Wang X., Cai J., 2023. Mapping and characterizing rock glaciers in the arid Western Kunlun Mountains supported by InSAR and deep learning. Journal of Geophysical Research: Earth Surface, 128, e2023JF007206. https://doi.org/10.1029/ 2023JF007206
- ISPRA, 2022. Dissesto idrogeologico in Italia: pericolosità e indicatori di rischio.
- Knight J., Mitchell W.A., Rose J., 2011. Geomorphological field mapping. In: J.F. Shroder (Ed.), Developments in Earth Surface Processes, 151-187. Elsevier, Amsterdam. https://doi.org/10.1016/B978-0-444-53446-0.00006-9
- Laimer H.J., 2021. Engineering geomorphology: a novel professional profile to face applied challenges in earth surface dynamics in mid-Europe. Earth Surface Processes and Landforms, 46, 2127-2135. https://doi.org/10.1002/esp.5176
- Lazos I., Papanikolaou I., Sboras S., Foumelis M., Pikridas C., 2022. Geodetic upper crust deformation based on primary GNSS and INSAR Data in the Strymon Basin, Northern Greece. Applied Sciences, 12, 9391. https://doi.org/10.3390/app12189391
- Lu P., Casagli N., Catani F., Tofani V., 2012. Persistent Scatterers Interferometry Hotspot and Cluster Analysis (PSI-HCA) for detection of extremely slow-moving landslides. International Journal of Remote Sensing, 33, 466-489. https://doi.org/10.1080/01431161.2010.536185
- Medici C., Becattini F., Dashwood C., Del Soldato M., Bianchini S., Bateson L., Novellino A., 2025. On the use of the EGMS data for studying landslides in Great Britain. In: Guzzetti F., Peruccacci S. (Eds), Earth Observation Applications to Landslide Mapping, Monitoring and Modeling, 71-86. Elsevier, Amsterdam. https://doi. org/10.1016/B978-0-12-823868-4.00005-2
- Meisina C., Zucca F., Notti D., Colombo A., Cucchi A., Savio G., Bianchi M., 2008. *Geological interpretation of PSInSAR data at regional scale.* Sensors, 8, 7469-7492. https://doi.org/10.3390/s8117469

- Montalti R., Solari L., Bianchini S., Del Soldato M., Raspini F., Casagli N., 2019. A Sentinel-1-based clustering analysis for geo-hazards mitigation at regional scale: a case study in Central Italy. Geomatics, Natural Hazards and Risk, 10, 2257-2275. https://doi.org/10.1080/19475705. 2019.1690058
- Murgia F., Bignami C., Brunori C.A., Tolomei C., Pizzimenti L., 2019. Ground deformations controlled by hidden faults: multi-frequency and multitemporal insar techniques for urban hazard monitoring. Remote Sensing, 11, 2246. https://doi.org/10.3390/rs11192246
- Navarro J.A., Tomás R., Barra A., Pagán J.I., Reyes-Carmona C., Solari L., Crosetto M., 2020. ADAtools: Automatic detection and classification of active deformation areas from PSI displacement maps. IS-PRS International Journal of Geo-Information, 9, 584. https://doi. org/10.3390/ijgi9100584
- Panizza M., 1996. *Environmental Geomorphology*. Elsevier, Amsterdam, 267 pp.
- Parenti C., Grassi F., Rossi P., Soldati M., Pattuzzi E., Mancini F., 2024. Synergistic use of synthetic aperture radar interferometry and geomorphological analysis in slow-moving landslide investigation in the Northern Apennines (Italy). Land, 13, 1505. https://doi.org/10.3390/ land13091505
- Pazzi V., Tanteri L., Bicocchi G., D'Ambrosio M., Caselli A., Fanti R., 2017. H/V measurements as an effective tool for the reliable detection of landslide slip surfaces: case studies of Castagnola (La Spezia, Italy) and Roccalbegna (Grosseto, Italy). Physics and Chemistry of the Earth, Parts A/B/C 98, 136-153. https://doi.org/10.1016/j.pce.2016.10.014
- Principi G., Bortolotti V., Chiari M., Cortesogno L., Gaggero L., Marcucci M., Saccani E., Treves, B., 2004. *The pre-orogenic volcano-sedimentary covers of the Western Tethys oceanic basin: a review.* Ofioliti, 29, 177-211.
- Solari L., Del Soldato M., Raspini F., Barra A., Bianchini S., Confuorto P., Crosetto M., 2020. Review of satellite interferometry for landslide detection in Italy. Remote Sensing, 12, 1351. https://doi.org/10.3390/ rs12081351
- Soldati M., Marchetti M. (Eds), 2017. Landscapes and landforms of Italy, World Geomorphological Landscapes. Book Series (WGLC). Springer, Cham, 539 pp. https://doi.org/10.1007/978-3-319-26194-2
- Strozzi T., Caduff R., Jones N., Barboux C., Delaloye R., Bodin X., Schrott L., 2020. Monitoring rock glacier kinematics with satellite synthetic aperture radar. Remote Sensing, 12, 559. https://doi. org/10.3390/rs12030559

- Tarquini S., Nannipieri L., 2017. The 10 m-resolution TINITALY DEM as a trans-disciplinary basis for the analysis of the Italian territory: current trends and new perspectives. Geomorphology, 281, 108-115. https://doi.org/10.1016/j.geomorph.2016.12.022
- Tiwari A., Shirzaei M., 2024. A novel machine learning and deep learning semi-supervised approach for automatic detection of InSAR-based deformation hotspots. International Journal of Applied Earth Observation and Geoinformation, 126, 103611. https://doi.org/10.1016/j.jag.2023.103611
- Tomás R., Pagán J.I., Navarro J.A., Cano M., Pastor J.L., Riquelme A., Casagli N., 2019. Semi-automatic identification and pre-screening of geological-geotechnical deformational processes using persistent scatterer interferometry datasets. Remote Sensing, 11, 1675. https://doi. org/10.3390/rs11141675
- Torre D., Galve J.P., Reyes-Carmona C., Alfonso-Jorde D., Ballesteros D., Menichetti M., Azañón J.M., 2024. Geomorphological assessment as basic complement of InSAR analysis for landslide processes understanding. Landslides, 21, 1273-1292. https://doi.org/10.1007/s10346-024-02216-w
- Trigila A., Iadanza C., Guerrieri L., 2007. Rapporto APAT 78/2007 Il Progetto IFFI (Inventario dei Fenomeni Franosi in Italia): metodologia, risultati e attività future. APAT, Roma, 382 pp.
- Vai G.B., Martini I.P. (Eds), 2001. Anatomy of an Orogen: the Apennines and Adjacent Mediterranean Basins. Springer, Dordrecht, 632 pp.
- Zucali M., Spalla M.I., 2011. Prograde lawsonite during the flow of continental crust in the Alpine subduction: strain vs. metamorphism partitioning, a field-analysis approach to inter tectonometamorphic evolutions (Sesia-Lanzo Zone, Western Italian Alps). Journal of Structural Geology, 33, 381-398. https://doi.org/10.1016/j.jsg.2010.12.006
- Zucali M., Spalla M.I., Gosso G., 2002. Strain partitioning and fabric evolution as a correlation tool: the example of the Eclogitic Micaschists Complex in the Sesia-Lanzo Zone (Monte Mucrone-Monte Mars, Western Alps, Italy). Schweizerische Mineralogische und Petrographische Mitteilungen, 82, 429-454.

(Ms. received 15 May 2025, accepted 24 September 2025)